Moments of the Raman spectrum of the two-dimensional Heisenberg antiferromagnet

Zhiping Liu and Efstratios Manousakis
Department of Physics, Center for Materials Research and Technology and Supercomputer Computations Research Institute, Florida State University, Tallahassee, Florida 32306
(Received 19 December 1990)

Using the spin-$\frac{1}{2}$ antiferromagnetic Heisenberg model on a square lattice, we calculate the first two cumulants of the Raman scattering intensity by the variational Monte Carlo method. We use a Jastrow variational wave function which includes spin-spin correlations and possesses antiferromagnetic long-range order. This wave function has been self-consistently obtained by minimizing the ground-state energy and by satisfying sum rules of the dynamical structure function; in addition, it gives values for the ground-state energy, the staggered magnetization, and the spin-wave velocity in good agreement with the results of other calculations. The values of the cumulants obtained by our variational Monte Carlo calculation, when extrapolated to the thermodynamic limit (using finite-size scaling forms suggested by spin-wave theory), are $M_1 = 3.69J$ and $M_2 = 0.72J$, in good agreement with those obtained by series expansion. Taking a value of $J = 1000\ \mathrm{cm}^{-1}$, our results also agree with the experimental data on La_2CuO_4.

I. INTRODUCTION

The isotropic two-dimensional (2D) spin-$\frac{1}{2}$ antiferromagnetic Heisenberg model (AFHM) is under intense theoretical investigation since a suggestion was made[1] that quantum spin fluctuations in the copper oxide planes of high-T_c materials may be responsible for their superconductivity. This model can be also obtained from Hubbard models in the strong-coupling limit and at half filling and describes the dynamics of the spin degrees of freedom of these copper oxides in the undoped insulating phase.[2] The temperature dependence of the correlation length as well as the dynamical correlations obtained from this model and the equivalent nonlinear σ model[3,4] are consistent with neutron scattering experiments[5] done on the undoped La_2CuO_4 by choosing a value of the antiferromagnetic coupling $J \sim 1000\ \mathrm{cm}^{-1}$.

In this paper we study cumulants of the intensity distribution of the Raman scattering from the undoped insulating quantum antiferromagnet La_2CuO_4. The in-plane quantum spin excitations are believed to be the reason for the broad peak around $3000\ \mathrm{cm}^{-1}$ in Raman scattering experiments.[6] The ratio of the width of this peak to its averaged frequency, if calculated using the spin-$\frac{1}{2}$ AFHM on the square lattice, is parameter free and provides a further test of the theoretical model underlying the spin fluctuations in the materials. However, this ratio calculated using conventional spin-wave theory,[7] even with magnon-magnon interaction being taken into account, is still nearly three times smaller than that observed experimentally. Therefore, other approaches beyond spin-wave theory which could capture such fluctuations are needed to study whether or not the magnitude of the width can be accounted for by such a rather simple model.

The series expansion method, which considers the Ising part of the Heisenberg Hamiltonian as unperturbed and the x-y part as a perturbation, has been used to calculate the various frequency moments of the Raman spectrum,[8] and a good agreement with experimental data was achieved. The uncertainty in the extrapolation procedure, used in the series expansion in order to reach the isotropic limit, is not entirely known due to the fact that the series converges quite slowly. This concern is also brought up in a recent exact diagonalization calculation[9] of the same quantities, in which the first moment is 11% smaller than that found by series expansion. The exact diagonalization is performed only on a 4×4 lattice and so it is not clear whether this discrepancy is due to finite-size effects or due to systematic errors in the series expansion calculation. Thus, additional calculations that support the results of the above two methods and clarify the situation further are desired.

In this paper we shall use a variational ground-state wave function of the spin-$\frac{1}{2}$ AFHM to calculate the first two cumulants of the Raman scattering intensity. This variational wave function has a form similar to those studied earlier by Marshall,[10] Horsch and von der Linden,[11] and Huse and Elser.[12] It is characterized by antiferromagnetic long-range order and takes into account spin-spin correlations. More recently, it has also been derived by an analytical approach[13] and we have optimized it by a variational Monte Carlo (VMC) calculation,[14] in which the long-range spin-spin correlations are taken into account in such a way that the wave function is consistent with the long-wavelength spin-wave excitations and the sum rules of spin dynamical structure function. The ground-state energy, staggered magnetization, and spin-wave velocity have been calculated[14] using this wave

function and agree fairly well with those obtained from other numerical methods.[15] Thus, the calculated values for the ground state properties of the spin-$\frac{1}{2}$ AFHM on the square lattice are reasonably accurate and such a variational wave function may be used to provide an independent calculation of the moments of the Raman scattering intensity.

The formulation and the way in which we implemented the variational calculation are explained in the next section. In Sec. III, the linear spin-wave[16] (LSW) theory is used to calculate the moments in order to have a qualitative understanding and obtain the finite-size dependence of the cumulants in the thermodynamic limit. The results obtained using the VMC method and their comparison with other calculations are given in Sec. IV.

II. FORMULATION

The Raman spectrum due to the interaction of the spin pairs with light is described by the following effective Hamiltonian:[7]

$$H_R = \sum_{<ij>} (\mathbf{E}_i \cdot \delta_{ij})(\mathbf{E}_s \cdot \delta_{ij}) \mathbf{S}_i \cdot \mathbf{S}_j, \tag{1}$$

where $\mathbf{E}_i$ and $\mathbf{E}_s$ are the electric-field vectors for the incident and scattered photons. δ_{ij} is a unit vector linking sites i and j and we have included only interactions between nearest neighbors. The scattered photon intensity distribution, at zero temperature, is given by the Fermi golden rule

$$I(\omega) = \sum_n |\langle \Psi_0 | H_R | \Psi_n \rangle|^2 \delta(\omega - (E_n - E_0)), \tag{2}$$

where $|\Psi_n\rangle$ corresponds to the nth eigenstate of the system (target) with eigenvalue E_n. It is clear that the calculation of the line shape $I(\omega)$ requires a full knowledge of the excited states $|\Psi_n\rangle$. However, the spectrum moments ρ_n defined below are quantities related to the ground-state properties only. We define

$$\rho_n = \int \omega^n I(\omega) d\omega. \tag{3}$$

The cumulants are defined as

$$(M_n)^n = \int (\omega - M_1)^n I(\omega) d\omega / \rho_0, \tag{4}$$

for $n > 1$, with $M_1 \equiv \rho_1/\rho_0$ and their values for $n = 1, 2$ have been measured using Raman scattering techniques[6] on undoped La_2CuO_4. Different cumulants are sensitive to different parts of the frequency spectrum and therefore contain complementary information.

We will use the 2D spin-$\frac{1}{2}$ AFHM given by

$$H = J \sum_{<i,j>} \mathbf{S}_i \cdot \mathbf{S}_j \tag{5}$$

to describe the dynamics of spin degrees of freedom of the undoped material. Here $\mathbf{S}_i$ is a spin-$\frac{1}{2}$ operator and the summation is over all nearest-neighbor pairs. After some algebraic manipulations, we write the first three moments as

$$\begin{aligned}
\rho_0 &= \langle \Psi_0 | H_R^2 | \Psi_0 \rangle = \sum_{i,j} \langle \Psi_0 | b_{i,i+\hat{x}} (b_{j,j+\hat{x}} - b_{j,j+\hat{y}}) | \Psi_0 \rangle, \\
\rho_1 &= \tfrac{1}{2} \langle \Psi_0 | [H_R, [H, H_R]] | \Psi_0 \rangle = \frac{J}{2} \sum_{i,j,l} \langle \Psi_0 | [[b_{i,i+\hat{x}}, b_{j,j+\hat{y}}], b_{l,l+\hat{x}}] | \Psi_0 \rangle, \\
\rho_2 &= -\langle \Psi_0 | [H, H_R]^2 | \Psi_0 \rangle = -J^2 \sum_{i,j} \langle \Psi_0 | [b_{i,i+\hat{x}}, b_{j,j+\hat{y}}]^2 | \Psi_0 \rangle,
\end{aligned} \tag{6}$$

where the bond operators $b_{i,i+\hat{x}}$ and $b_{i,i+\hat{y}}$ denote $\mathbf{S}_i \cdot \mathbf{S}_{i+\hat{x}}$ and $\mathbf{S}_i \cdot \mathbf{S}_{i+\hat{y}}$, respectively. We have considered only the scattering geometry of the B_{1g} symmetry, i.e., the incident light $\mathbf{E}_i$ and the scattered light $\mathbf{E}_s$ are polarized along the direction having an angle 45^0 with respect to the $\hat{x}$ axis. The unit vectors $\hat{x}$ and $\hat{y}$ are along the directions of the Cu–O bond in the plane. We used the fact that the expectation values of $b_{i,i+\hat{x}} b_{j,j+\hat{x}}$ and $b_{i,i+\hat{y}} b_{j,j+\hat{y}}$ are equal due to the rotational invariance of the ground-state wave function in the coordinate space. Because we are merely interested in calculating ρ_1/ρ_0 and ρ_2/ρ_0, the amplitudes of $\mathbf{E}_i$ and $\mathbf{E}_s$ are set to unity in the above expressions.

A good approximation to the ground-state wave function of the AFHM was found in Refs. 13 and 14. This wave function can be written in the following form:

$$|\Psi_0\rangle = \exp\left(-\frac{1}{2} \sum_{i<j} u_{ij}\, \hat{\sigma}_i^z \hat{\sigma}_j^z\right) |\phi\rangle, \tag{7}$$

where

$$|\phi\rangle \equiv \frac{1}{\sqrt{2^N}} \sum_c (-1)^{L(c)} |c\rangle, \tag{8}$$

where N is the number of sites and the sum is over all possible spin configurations c of the lattice and $L(c)$ is the number of "up" spins in one sublattice contained in the configuration c; $\hat{\sigma}_i^z$ is the spin operator with eigenvalues $+1$ for up spins and -1 for down spins. The state $|\phi\rangle$ is the Néel state along the $\hat{x}$ axis in spin space, because it can be written as $|\phi\rangle = \prod_{\mathbf{r}\in A} |\mathbf{r}, +\rangle \prod_{\mathbf{r}\in B} |\mathbf{r}, -\rangle$ where the states $|\mathbf{r}, +\rangle$ and $|\mathbf{r}, -\rangle$ are the eigenstates of $\hat{\mathbf{S}}_{\mathbf{r}}^x$ and A and B represent the two sublattices. The function u_{ij}

was obtained by "paired-magnon analysis"[3] and is given by

$$u_{ij}^{\mathrm{PMA}} \equiv \frac{1}{N}\sum_{\mathbf{k}}\left(\sqrt{\frac{1+\gamma_{\mathbf{k}}}{1-\gamma_{\mathbf{k}}}}-1\right)e^{i\mathbf{k}\cdot(\mathbf{r}_i-\mathbf{r}_j)}, \tag{9}$$

where $\gamma_{\mathbf{k}} = \frac{1}{2}[\cos(k_x)+\cos(k_y)]$. The wave function (7) has the Jastrow form which takes into account the spin-spin correlations arising from the constraint that two spins cannot occupy the same site, analogous to the hard-core interaction in the liquid ^{4}He. It has been optimized by a VMC calculation,[14] and the optimal values of variational parameters are $u(1,0) = u(0,1) = 0.612$, $u(1,1) = 0.34$, and the long-range tail $u_{ij} = 1.22u_{ij}^{\mathrm{PMA}}$ for $|\mathbf{r}_{ij}| \equiv \sqrt{(x_i-x_j)^2+(y_i-y_j)^2} \geq 2$; the factor 1.22 makes the wave function consistent with sum rules for the spin dynamical structure function. The values of the ground-state energy per site, the staggered magnetization, and the spin-wave velocity obtained with this wave function are $-0.6637(2), 0.349(2)$, and $1.22\sqrt{2}Ja$, respectively, and they are in good agreement with other calculations.[2] This optimal wave function will be used next in the calculations of the moments of the Raman spectrum given by Eqs. (6).

Let us consider the calculation of the nth moment ρ_n. Using the variational wave function (7), we obtain

$$\rho_n = \frac{\sum_c P(c)Q(c)}{\sum_c P(c)}, \tag{10}$$

where

$$P(c) = \exp\left(-\sum_{i<j}u_{ij}\sigma_i^z(c)\sigma_j^z(c)\right), \tag{11}$$

$$Q(c) = \sum_{c'}(-1)^{L(c)-L(c')}\exp\left(\frac{1}{2}\sum_{i<j}u_{ij}(\sigma_i^z(c)\sigma_j^z(c)-\sigma_i^z(c')\sigma_j^z(c'))\right)\langle c'|\hat{Q}|c\rangle. \tag{12}$$

In our case $\hat{Q}$ represents the operators which are combinations of bond operators and determine the moments in Eqs. (6). Following standard Monte Carlo techniques, we first need to generate spin configurations c distributed according to the probability function $P(c)$. The expectation value of $Q(c)$ is then obtained by the summation over such configurations. For a given configuration c, one needs to perform the summation in (12) only over those configurations c' that give nonzero matrix elements $\langle c'|\hat{Q}|c\rangle$.

To calculate the matrix elements, we make use of diagrammatic representations and consider the symmetries of the ground-state wave function in order to simplify the algebra. The basic element of these diagrams is a bond with an index i, which connects two nearest-neighbor sites and represents the bond operators $b_{i,i+\hat{x}}$ and $b_{i,i+\hat{y}}$ for a horizontal and vertical bond, respectively. A summation over all lattice sites i is implied. Therefore, each term contributing to ρ_n is a sum of expectation values of products or multicommutators of such bond operators.

In Figs. 1(a)–1(c), we give the terms contributing to ρ_0, ρ_1, and ρ_2, respectively. Each term in Fig. 1(a) is an expectation value of the product of two bonds. In Fig. 1(b) each term refers to the average value of a double commutator of the form $[[\hat{\alpha},\hat{\beta}],\hat{\tau}]$, where $\hat{\beta}$ is the vertical bond and $\hat{\alpha}$ the one connected to the vertical bond. Each term in the second moment ρ_2 consists of four bonds, and is expressed as the product of two right angles [see Fig. 1(c)]. Each such right angle is a commutator of two bonds of the form $[b_{i,i+\hat{x}}, b_{i,i+\hat{y}}]$, where the horizontal bond is always the first and the vertical bond second.

The symmetries of the wave function (7) greatly reduce

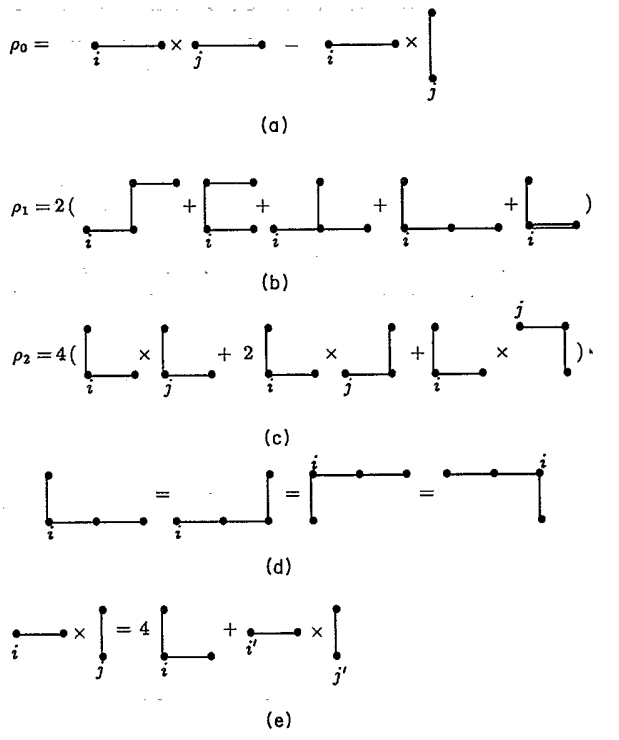

FIG. 1. (a)–(c) Diagrammatic representation of the first three moments; see text for details. (d) Due to rotational symmetries these four diagrams give the same contribution. (e) The second term of ρ_0 can be split into four connected bonds (giving the same expectation value) and a product of two disconnected bonds. The indices i' and j' imply summation over the lattice with the restriction that the two bonds have no common site.

the number of diagrams to be computed. For example, the probability function $P(c)$ given by (10) is invariant under certain transformations of the configuration c. Diagrams which differ by rotations give the same contribution to the moments, as illustrated in Fig. 1(d). One has to take particular care when calculating ρ_0 and ρ_2, which involve connected as well as disconnected bonds. Each term in Fig. 1(a) and 1(c) can be split into connected and disconnected bonds, as shown in Fig. 1(e). The number of the connected diagrams to be calculated can be again reduced using such symmetries, as demonstrated in Fig. 1(e).

The moments ρ_0, ρ_1, and ρ_2 are proportional to the number of sites N in the $N \to \infty$ limit. Let us consider ρ_0, for example. Due to the translational invariance, the summation over i, j can be replaced by a factor N times the sum over all possible values of $\mathbf{r}_{ij}$. The expectation values of $b_{i,i+\hat{\mathbf{x}}} b_{j,j+\hat{\mathbf{x}}}$ and $b_{i,i+\hat{\mathbf{x}}} b_{j,j+\hat{\mathbf{y}}}$, when $|\mathbf{r}_{ij}|$ is large, become $\langle\Psi_0|b_{i,i+\hat{\mathbf{x}}}|\Psi_0\rangle\langle\Psi_0|b_{j,j+\hat{\mathbf{x}}}|\Psi_0\rangle$ and $\langle\Psi_0|b_{i,i+\hat{\mathbf{x}}}|\Psi_0\rangle\langle\Psi_0|b_{j,j+\hat{\mathbf{y}}}|\Psi_0\rangle$, respectively. Since the symmetries of the wave function imply that $\langle\Psi_0|b_{j,j+\hat{\mathbf{x}}}|\Psi_0\rangle = \langle\Psi_0|b_{j,j+\hat{\mathbf{y}}}|\Psi_0\rangle$, these pieces cancel at sufficiently large $|\mathbf{r}_{ij}|$. There are the remaining parts for finite values of $|\mathbf{r}_{ij}|$, which when summed over all values of $\mathbf{r}_{ij}$, give a contribution of order unity.

III. MOMENTS FROM SPIN-WAVE THEORY

To first obtain a qualitative picture, we present here the optical moments of the spin-$\frac{1}{2}$ AFHM using linear spin-wave theory.[16] By means of Holstein-Primakoff transformation we can express the Hamiltonians H_R and H in terms of two kinds of bosonic spin operators for each sublattice. We keep only quadratic operator terms and perform the Bogoliubov canonical transformation to rewrite these Hamiltonians using magnon creation and annihilation operators. The spin-wave ground state is used to evaluate the expectation values defined in Eqs. (6). We find

$$\rho_0^{\mathrm{LSW}} = \sum_{\mathbf{k}} \frac{(\cos k_x - \cos k_y)^2}{4(1-\gamma_{\mathbf{k}}^2)},$$
$$\rho_1^{\mathrm{LSW}} = \sum_{\mathbf{k}} J \frac{(\cos k_x - \cos k_y)^2}{\sqrt{1-\gamma_{\mathbf{k}}^2}}, \qquad (13)$$
$$\rho_2^{\mathrm{LSW}} = \sum_{\mathbf{k}} 4(\cos k_x - \cos k_y)^2 J^2.$$

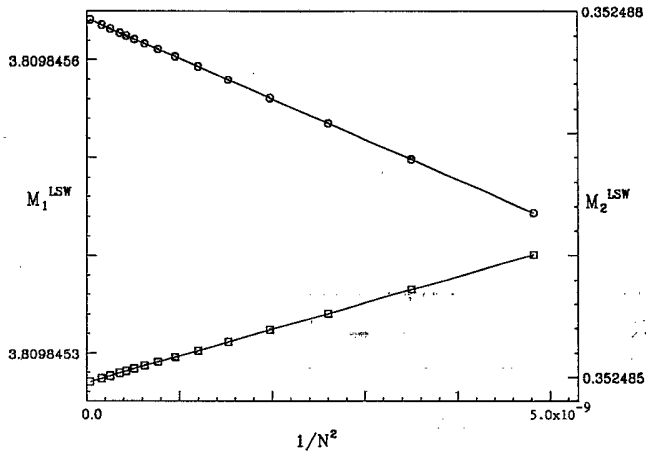

FIG. 2. The first two cumulants obtained from the LSW theory calculation. The open circles and squares are the values of M_1 and M_2 for lattices of sizes ranging from 120×120 to 400×400. The left ordinate is scaled for M_1^{LSW} and the right ordinate is for M_2^{LSW}. The solid lines are straight joining of these points. This demonstrates that the finite-size corrections to M_1 and M_2 are of order $1/N^2$ within LSW theory.

These equations hold for the B_{1g} symmetry only. In lattices of finite size, $\mathbf{k}$ takes discrete values and the summation over $\mathbf{k}$ can be carried out numerically for large size lattices so that the leading finite-size corrections can be found. Figure 2 demonstrates that the first two cumulants $M_1^{\mathrm{LSW}}, M_2^{\mathrm{LSW}}$ are linear functions of N^{-2} at large N. The values extrapolated to infinite N are given in Table I.

Equations (13) can also be derived using a somewhat different formalism. Elliott and Thorpe[7] applied the Green's function technique to study the AFHM and used the Néel state as the approximate ground state to evaluate the inhomogeneous term of the equation of motion. We find that the expressions for the moments obtained from their unperturbed Green's function are different from the above expressions obtained from LSW theory by a factor of $1/\sqrt{1-\gamma_{\mathbf{k}}^2}$. However, when we used the spin-wave ground state to calculate the inhomogeneous term, we found the same equations as (13).

Taking the magnon-magnon interactions into account in the Green's function approach, Elliot and Thorpe found that the line shape changes to a distribution

TABLE I. Comparison with other calculations. Experimental values are taken from Ref. 8

	M_1	M_2	M_2/M_1
Néel ground state	$4J$	0	0
LSW	$3.809\,845J$	$0.352\,486J$	0.093
Exact diagonalization (4×4)	$3.244J$	$0.797J$	0.246
Series expansion	$3.58(6)J$	$0.81(5)J$	0.23
This work	$3.69(2)J$	$0.72(5)J$	0.20(1)
Experimental values	3700(50) (cm^{-1})	1050(100) (cm^{-1})	0.28

peaked around $2.7J$ and the ratio of the second cumulant to the first one is 0.11, which is not significantly different from the LSW value of 0.09 and nearly three times smaller than the experimental value[8] of 0.28.

IV. VARIATIONAL CALCULATION

Our numerical calculations were performed on square lattices of sizes up to 16×16 with periodic boundary conditions. Note that the Heisenberg Hamiltonian conserves the total magnetization, which is zero[10] for the case of the ground state, and the calculation is restricted to this subspace. We checked our program by setting $u_{ij} = 0$ in the probability function (10), which means that all the configurations were sampled with the same probability. This corresponds to the Néel state along the $\hat{\mathbf{x}}$ direction in the spin space and the calculation of the moments can be carried out analytically giving $\rho_0 = N/8, \rho_1 = N/2$, and $\rho_2 = 2N$. Our program reproduces these values within error bars.

In Fig. 3(a) we present the numerical values of the first cumulant M_1 on different size lattices. The leading finite-size correction is of order N^{-2} as predicted by the LSW theory discussed in the previous section. The results obtained by our VMC calculation are shown by the open squares. The solid straight line is a least-squares fitting which gives $M_1 = 3.69(2)J$ in the limit of infinite N. The fit includes the results for lattices of sizes $6^2, 8^2, 10^2, 12^2$, and 16^2. In Fig. 3(b) we compare our VMC results with those obtained by the exact diagonalization[9] on a 4×4

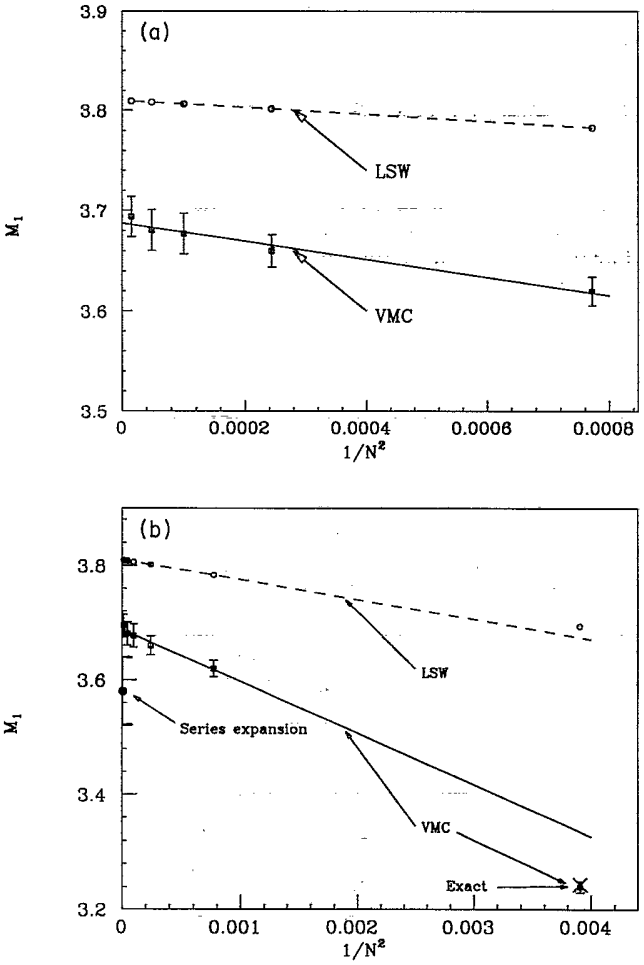

FIG. 3. (a) The first cumulant M_1 is plotted as a function of N^{-2} for square lattices of $N = L \times L$ spins. The open squares are the results of VMC and the open circles are the results of LSW theory. The lattice sizes correspond to L=6,8,10,12,16. Both solid and dashed straight lines are obtained by a least-squares fitting. (b) Comparison with other calculations. The result of the exact diagonalization on the 4×4 lattice is shown by the cross and the result of the series expansion is shown by the solid circle. The dashed and solid straight lines are the same fitting lines as in (a).

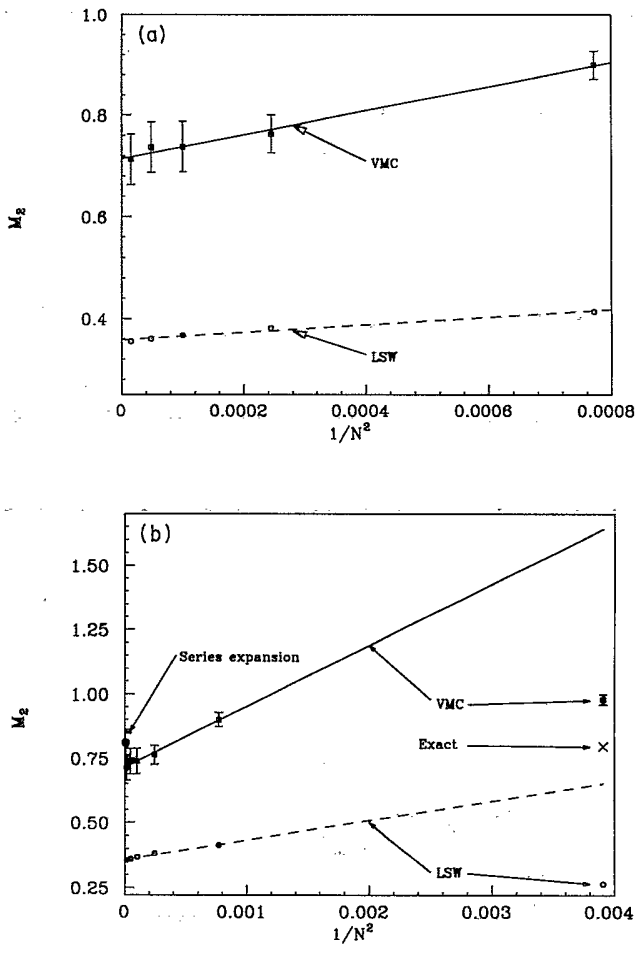

FIG. 4. (a) The results for the second cumulant M_2 as a function of N^{-2} obtained with the VMC calculation are shown by the open squares fitted by a solid straight line. The results obtained by LSW theory are shown by the circles fitted by a dashed line. The lattices used are $L \times L$ with $6 \leq L \leq 16$ (b) Comparison with other calculations. The result of the exact diagonalization on the 4×4 lattice is shown by the cross and the result of the series expansion is shown by the solid circle. Notice that the values obtained on a 4×4 lattice from both VMC calculation and LSW theory are far off the fitting lines.

lattice and by the series expansion.[8] The solid straight line is the same as that of Fig. 3(a), namely, obtained by excluding the result for the 4×4 lattice from the fitting. Our value for M_1 on a 4×4 lattice is $3.24J \pm 0.01$ which agrees with the value of $3.244J$ of the exact diagonalization (cross). Thus it can be seen that M_1 has considerable finite-size corrections when calculated on a 4×4 lattice. Our value extrapolated to the infinite N limit is in reasonable agreement with the result of the series expansion [solid circle in Fig. 3(b)]. Therefore, we conclude that the earlier difference between series expansion and exact diagonalization calculations mentioned in the Introduction is mainly due to the finite-size effects in the latter calculation.

The magnitude of the second cumulant M_2, which measures the width of the peak in the Raman scattering intensity, displays the role of the quantum spin fluctuations; M_2 is zero when calculated using (6) and the Néel ground state to obtain the expectation value. Figure 4(a) shows the results for M_2 obtained by our VMC calculation (open squares) and LSW theory (open circles). The extrapolated values are given in Table I. The error bars in this case are larger than in the case of M_1, mainly because of the error propagation from all three moments. In Fig. 4(b) we compare the results of our VMC calculation to those obtained by the exact diagonalization on the 4×4 lattice and by the series expansion. We did not include the point obtained on the 4×4 lattice in fitting the data, because it falls far off the fitting line. This behavior also appears in the LSW calculation shown by the open circles fitted by the dashed line.

The comparison with other calculations in Table I indicates the good agreement between the VMC results and those found by the series expansion method.[8] Comparing our value for $M_1 = 3.69(2)J$ and the experimental value listed in Table I, we obtain the antiferromagnetic exchange parameter $J = 1000 \pm 50$ cm^{-1}, indistinguishable from the value obtained by the series expansion within the errors. On the other hand, in order to fit the temperature dependence of the in-plane spin correlation length of stoichiometric La_2CuO_4 (the sample with Néel temperature 245 K) from the neutron scattering experiment, a value of $J = 1030$ cm^{-1} was used[2] in the quantum Monte Carlo calculation of the spin-$\frac{1}{2}$ AFHM on the square lattice. The same value of J can be used to calculate the spin-wave velocity given by $1.22\sqrt{2}Ja$, which gives $c \simeq 0.81$ eV Å, in good agreement with the value inferred from the neutron scattering experiment.[17] The consistency of these results indicates that the spin-$\frac{1}{2}$ AFHM may be relevant to the physics behind the spin fluctuations in the undoped La_2CuO_4. Lastly, we believe that the variational wave function (7) captures the basic nature of the spin fluctuations in the Heisenberg model.

ACKNOWLEDGMENTS

We wish to thank Paul Oppenheimer (Thinking Machines Corporation) for useful assistance and ideas on programming on the Connection Machine. This work was supported in part by the Supercomputer Computations Research Institute of Florida State University which is partially funded by the U. S. Department of Energy under Contract No. DE-FC05-85ER-250000 and in part by the U. S. Defense Advanced Research Projects Agency sponsored Florida Initiative in Advanced Microelectronics and Materials under Grant No. MDA972-88-J-1006.

[1] P. W. Anderson, Science **235**, 1196 (1987).
[2] E. Manousakis, Rev. Mod. Phys. (to be published).
[3] E. Manousakis and R. Salvador, Phys. Rev. Lett. **62**, 1310 (1989).
[4] S. Chakravarty, B. I. Halperin, and D. R. Nelson, Phys. Rev. Lett. **60**, 1057 (1988); Phys. Rev. B **39**, 2344 (1989); S. Tyc, B. I. Halperin, and S. Chakravarty, Phys. Rev. Lett. **62**, 835 (1989).
[5] Y. Endoh *et al.*, Phys. Rev. B **37**, 7443 (1988).
[6] K. B. Lyons *et al.*, Phys. Rev. B **39**, 9693 (1989); S. Sugai, *ibid.* **38**, 6436 (1988).
[7] J. B. Parkinson, J. Phys. C **2**, 2012 (1969); J. R. Elliott and M. F. Thorpe, *ibid.* **2**, 1630 (1969).
[8] R. Singh, P. Fleury, K. Lyons, and P. Sulewski, Phys. Rev. Lett. **62**, 2736 (1989).
[9] E. Dagotto and D. Poilblanc, Phys. Rev. B **42**, 7940 (1990); E. Gagliano and S. Bacci, *ibid.* **42**, 8772 (1990).
[10] W. Marshall, Proc. R. Soc. (London) A **232**, 48 (1955).
[11] P. Horsch and W. von der Linden, Z. Phys. B **72**, 181 (1988).
[12] D. A. Huse and V. Elser, Phys. Rev. Lett. **60**, 2531 (1988).
[13] E. Manousakis, Phys. Rev. B **40**, 4904 (1989).
[14] Z. Liu and E. Manousakis, Phys. Rev. B **40**, 11 437 (1989).
[15] J. Carlson, Phys. Rev. B **40**, 846 (1989); N. Trivedi and D. M. Ceperley, *ibid.* **40**, 2747 (1989).
[16] P. W. Anderson, Phys. Rev. **86**, 694 (1952); R. Kubo, *ibid.* **87**, 568 (1952); T. Oguchi, *ibid.* **117**, 117 (1960).
[17] G. Aeppli *et al.*, Phys. Rev. Lett. **62**, 2052 (1989).